QUARTERLY OF APPLIED MATHEMATICS
VOLUME LXII, NUMBER 2
JUNE 2004, PAGES 323–335

MAPPING ONTO THE PLANE OF A CLASS OF CONCAVE BILLIARDS

BY

RICHARD L. LIBOFF

Schools of Electrical Engineering and Applied Physics and Center for Applied Math, Cornell University, Ithaca, NY 14853

Abstract. Three results are reported in this work. The first addresses the four 'elemental-polygon' billiards with sides replaced by circular non-overlapping concave elements. Any orbit of the resulting concave billiard is mapped onto a trajectory in the plane that is shown to diverge from the trajectory of the related polygon billiard. This mapping permits application of Lyapunov exponents relevant to an unbounded system to be applied to the bounded concave elemental polygon-billiards. It is shown that Lyapunov exponents for concave elemental polygon-billiards go to zero as the curvature of the concave billiard segments go to zero. The second topic considers the quantum analogue of this problem. A conjecture is introduced which implies that a characteristic quantum number exists below which the adiabatic theorem applies and above which quantum chaos ensues. This parameter grows large as side curvature of the given billiard grows small. Lastly, a correspondence property between classical and quantum chaos for the concave elemental-polygon billiards is described.

1. Introduction. It has long been established [1-5] that in the classical polygon-billiard problem, four polygons are integrable in the sense that only these polygon billiards permit the billiard trajectory to be mapped onto a torus. These 'elemental' polygons: π $(1/4, 1/4, 1/2); \pi/3$ $(1, 1, 1); \pi/6$ $(1, 2, 3)$; $\pi/2(1, 1, 1, 1)$ are distinguished in the quantum domain as well [6,7]. Namely, it is for these and only these polygons (concave and convex) that respective ground states are analytic in the closed domains of respective billiards.

In the present work we consider the 'concave-elemental' polygon billiards. Each such polygon has its straight edges replaced by symmetrically situated circular concave segments that do not overlap within the polygon, such that the point of maximum depression of any such circular-arc segment corresponds to the center of the respective edge [8]. For a square billiard of edge-length a, the maximum depression is 0.207 a, or equivalently, 0.293 ρ, where ρ is the radius of curvature of the circular segment (see Appendix). Such

Received August 22, 2002.
2000 *Mathematics Subject Classification.* Primary 52Bxx.

billiards are important to the study of classical billiard chaos [8,9-11] and are known individually to be chaotic [12]. In this work, a procedure is introduced that maps the concave elemental-polygon billiard orbit onto a trajectory in the plane which is noted to diverge from the trajectory of the related straight-edged polygon billiard. For an unbounded system, Lyapunov exponents are defined in terms of the logarithmic ratio of displacement elements in the limit that time goes to infinity [10]. For bounded dynamical systems, Lyapunov exponents are defined in terms of a sequence of logarithmic ratio of displacement elements [13,14]. The present mapping permits application of Lyapunov exponents relevant to an unbounded system to be applied to the bounded concave elemental-polygon billiards. With this observation at hand, it is argued that Lyapunov exponents for concave elemental-polygon billiards tend continuously to zero with the curvature of the concave billiard segments. In a closely allied work of Heller et al. [15], estimates were made of energy dissipation rates corresponding to deformation of a billiard boundary. In another related study, Casati and Prosen [16] concluded that irrational triangular billiards (i.e., angles irrational with π) are mixing.

A Hamiltonian system with N degrees of freedom is integrable providing it has N constants of motion [17]. These constants restrict the motion of the system trajectory to an N-dimensional surface in $2N$-dimensional phase space. These surfaces are invariant tori. When less than this number of constants exist, the motion is nonintegrable. In such cases, it may be the case that approximate constants exist which, on a short time scale, confine dynamics to regions of phase space 'near' pertubatively distorted tori. Such motion has been described as being on a 'vague' torus [18-20]. For two-dimensional configurations studied in the present work, the energy is the only constant, and the related motion is nonintegrable and chaotic [1-3]. Whereas a number of works have addressed non-integrable billiards [21-26], for the most part, such studies do not examine mapping of these billiards onto the plane.

2. The Mapping. The fundamental element of the mapping onto the plane for any of the elemental polygon-billiards is shown in Fig. 1a, and is relevant to a side element of any of these billiards. In this procedure, the incident trajectory and concave element on which the trajectory is incident are reflected through the line connecting end points of the concave element. The reflected component of the trajectory is then completed in the reflected domain. Note that the lines connecting end points of the concave segments ('diameter') comprise the related straight-sided elemental polygon array. The 'lens' angle θ_L, measured from the lens surface-normal at the point of contact, and the 'plane' angle θ_P, measured from the normal to the plane at the point of contact, are shown in Fig. 1a. To prove that $\theta_P > \theta_L$, we refer to the scattering triangle configuration shown in Fig. 1b,c. With this figure, we see that $\theta_P - \theta_L$ is an acute angle of the inscribed triangle which establishes the inequality.

We recall that the phase space of a billiard is composed of the contact point of a trajectory and the angle between the normal to the surface and the incident trajectory at the point of contact (e.g., θ_P for a straight edge). In a 'reduced' diagram, incident and reflected trajectories on a lens element are brought to a common reflection point on the diameter line of the lens as in Fig. 1c. Motion in the reduced frame may be mapped

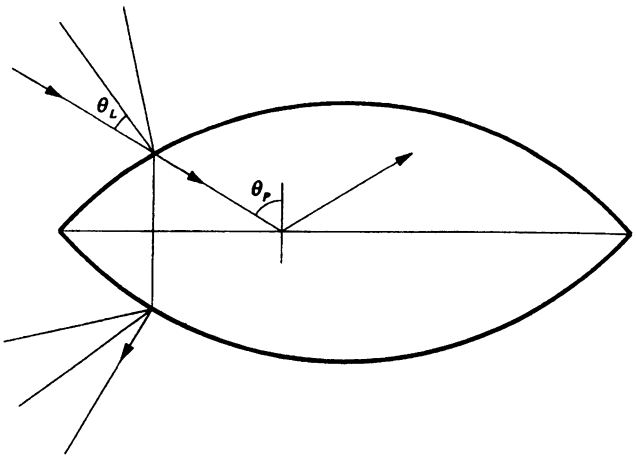

(a)

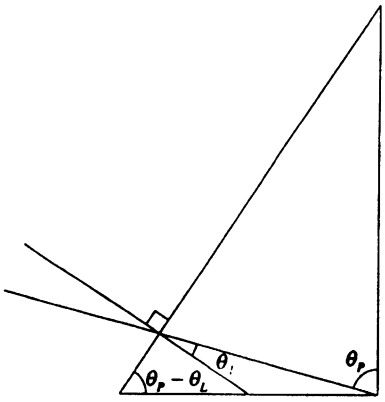

(b)

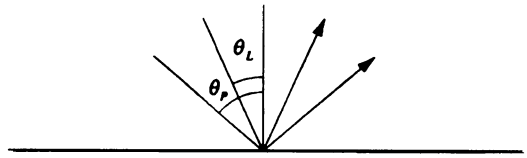

(c)

FIG. 1. Basic elements of the mapping: (a) Draw a line, P, which connects end points of the lens element. Consider a trajectory which is incident on the concave element. Reflect the incident trajectory and concave element upon which it is incident through the line P and complete the reflection in the reflected domain. Note that reflection back through P gives the bounce trajectory in the starting domain. The angles θ_P and θ_L are shown. (b) Triangle configurations corresponding to the scattering of Fig. (a), demonstrating that the angle $\theta_P - \theta_L$ is an acute angle of the inscribed right triangle which establishes the inequality $\theta_P > \theta_L$. (c) The angles θ_P and θ_L in the reduced zone picture.

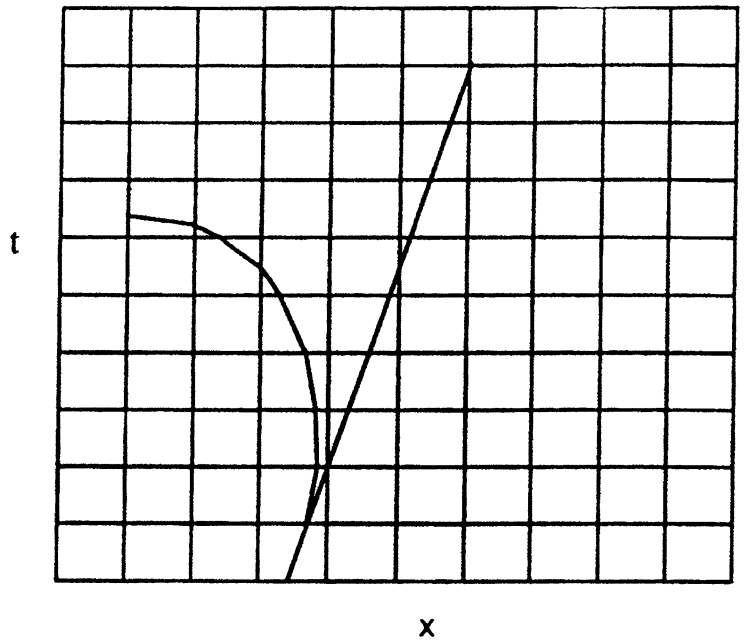

FIG. 2. Displacement-time trajectories in the extended reduced-zone picture, exhibiting divergence of the trajectory of the concave billiard from that of the square billiard.

onto a torus. From the construction it is noted that this motion is chaotic. Note that the motion in the reduced frame preserves phase-space coordinate values.

Application of this procedure to the concave square billiard is shown in Fig. 2 in which the extended motion in the plane for the square billiard and its concave image in the reduced frame are shown. With this diagram, one notes the implied divergence of adjacent trajectories for the concave square billiard. This procedure applies to any of the remaining three concave elemental polygons as well.

3. Lyapunov Exponents. Lyapunov exponents for an unbounded single-particle system are defined as follows [9-11]. Consider two neighboring trajectories, $\mathbf{r}_1(t)$ and $\mathbf{r}_2(t)$, and the difference of their incremental displacements,

$$\Delta\mathbf{r}_1(t) - \Delta\mathbf{r}_2(t). \tag{1a}$$

Let $\mathbf{e}_i$, $(i = 1, 2)$ denote unit orthogonal vectors in the plane. The related components of incremental displacement are given by

$$d_t^{(i)} = \mathbf{e}_i \cdot \Delta\mathbf{r}(t). \tag{1b}$$

Consider the form

$$L^{(i)} \equiv \ln\left(\frac{d_t^{(i)}}{d_0^{(i)}}\right). \tag{2}$$

The Lyapunov characteristic exponent may be written

$$\lambda^{(i)} = \lim_{t\to\infty} \frac{1}{t} L^{(i)}(t). \tag{3}$$

The preceding expression is invalid for a finite system. However, with the mapping described above, in which trajectories of the concave elemental polygon-billiard are mapped onto the plane, the expression (3) becomes appropriate to these finite configurations. That is, for such finite systems, (3) is evaluated with respect to the extended motion in the plane.

It is well known that the concave billiard is chaotic [12]. It follows that in the extended equivalent motion, the Lyapunov exponent, $\lambda^{(i)} > 0$. Let ϵ denote the curvature of a side element (i.e., $\epsilon \propto 1/\rho$). As $\epsilon \to 0$, the concave billiard approaches the unperturbed straight billiard, so that in this limit, $d_t^{(i)}/d_0^{(i)} \propto t$, and $\lambda^{(i)} \to 0$. This conclusion is corroborated in closely allied works [27,28].

4. Quantum-Billiard Chaos. Quantum chaos partitions into three classes [29]: (a) quantized chaos, (b) semi-quantum chaos, and (c) true quantum chaos. The first class, in which one examines classically chaotic systems in the semiclassical regime limit, has been labeled 'quantum chaology' [30]. In semi-quantum chaos, a subcomponent of a quantum mechanical system exhibits chaotic behavior. In true quantum chaos, the entire quantum system is chaotic and exhibits exponential sensitivity. It has been argued that a system of coupled phase oscillators is an example of this class of chaos [31]. In the quantum analogue of these billiard problems, one examines solution of the Helmholtz equation [32], satisfying Dirichlet boundary conditions, in a convex two-dimensional domain in the plane [33-37]. We are concerned with the quantum chaology of these systems. In Fig. 2, we see that the augmented trajectory of the concave elemental polygon billiard grows uniformly contiguous to the corresponding linear trajectory of the elemental polygon billiard with reduction of curvature of side elements. The pre-chaotic interval (i.e., the interval for chaos to develop) grows large as the side curvature grows small. However, for any curvature, no matter how small, chaotic behavior eventually emerges.

Quantum states of high quantum number may be associated with long-time behavior. Eigenenergies for the quantum billiard are positive and grow with increase of quantum number. Stationary states carry the time-dependent factor $\exp(-i\omega_{\mathbf{n}}t)$, where $E_{\mathbf{n}} \equiv \hbar\omega_{\mathbf{n}}$, and $\mathbf{n}$ denotes a two-integer pair. As noted below, for any of the elemental quantum billiards, $\omega_{\mathbf{n}} \sim n^2\omega_0$. It follows that at any time, t, for sufficiently large n, the time-dependent factor goes as $\exp(-i\omega_0 n^2 t)$, so that the wavefunction , $\Psi_{\mathbf{n}}(\mathbf{r}, t)$, has effective long-time dependence. As quantum billiard chaos is defined in the high quantum-number domain, it is conjectured that for such systems a characteristic quantum number $\mathbf{n}_c$ exists, above which quantum chaos develops. Relevant to the present study, one may infer that $\mathbf{n}_c$ grows large as side curvature grows small. For quantum numbers less than $\mathbf{n}_c$, the adiabatic theorem applies [32]. We recall that in an adiabatic change of, say, the square billiard to the concave square billiard, the $\mathbf{n}^{th}$ wavefunction of the square billiard goes to the $\mathbf{n}^{th}$ wavefunction of its concave image for $\mathbf{n} < \mathbf{n}_c$. With Courant's nodal partitioning theorem [30], one may conclude that the nodal structure of the given

eigenstate maintains its topological character during this transformation, for eigenstates in the quantum-number interval $\mathbf{n} < \mathbf{n}_c$. For larger eigenvalues, states of the perturbed system mix, resulting in chaotic behavior [39,40].

This conjecture finds corroboration in numerical study of the perturbed rectangular quantum billiard. In the perturbed boundary, the shorter sides of the rectangle are replaced by elliptical sections with sufficiently small minor-to-major axis ratio, α. The classical chaotic property of this billiard is known [29]. In the numerical program, the Helmholtz equation is given by

$$\epsilon\nabla^2\varphi(x,y) + \kappa\varphi(x,y) = 0, \tag{4}$$

where ϵ is a constant introduced for numerical study. In the present work, it is set equal to 0.1. In Figs. 3 and 4, the second eigenstate of the Laplacian is shown for both the unperturbed, $\kappa \cong 3.8383$, and perturbed rectangle, $\kappa \cong 4.6273$, respectively, in which it is seen that there is virtually no change in the nodal line of this eigenstate. In Figs. 5 and 6, the 35th eigenstate is shown for both the unperturbed, $\kappa \cong 55.1033$, and perturbed rectangle, $\kappa \cong 63.6661$, respectively, in which it is seen that there is a loss of symmetry of the nodal structure of the unperturbed eigenstate in the perturbed configuration.

Numerical work implies further that the critical eigenvalue, above which the symmetry of the nodal pattern of an unperturbed system is lost in the perturbed system, grows large as α grows small. These observations lend consistency to the given conjecture.

The long-time development for classical chaos for small side curvature of the concave elemental billiards corresponds in the quantum cases to the relatively large value of $\mathbf{n_c}$ for these configurations. With our preceding description, this quantum property may be associated with effective long-time quantum behavior, parallel to the classical property thereby establishing another element of classical-quantum correspondence [40].

5. Elemental Billiard Eigenproperties. Eigenenergies of the equilateral triangle billiard [33] go as $n^2 + n'^2 - nn'$, which in the large quantum-number domain, grow as n^2. In this latter expression, n and n' are positive integers that satisfy simple constraints, namely: $n + n' = 3s; n' \neq 2n; n \neq 2n'$, where s is an integer. Consider one of the right triangles formed by bisecting the equilateral triangle, *viz.*,$(\pi/6)$ $(1, 2, 3)$. By the process of odd reflection [37], eigenstates of this triangular quantum billiard are produced that have the same eigenenergies as the equilateral triangle quantum billiard. Together with well-known results for the square quantum billiard, we may conclude that eigenenergies of all four elemental-polygon quantum billiards are integers and grow as [2] and separate, respectively, as n, in the classical limit. It follows that eigenenergies of each of the four elemental quantum billiards grow as sE_1, where s is a positive integer and E_1 is a constant energy.

6. Conclusions. In conclusion, a procedure is introduced that maps the concave elemental polygon billiard orbit onto a trajectory in the plane, which in turn permits application of Lyapunov exponents relevant to an unbounded system to be applied to

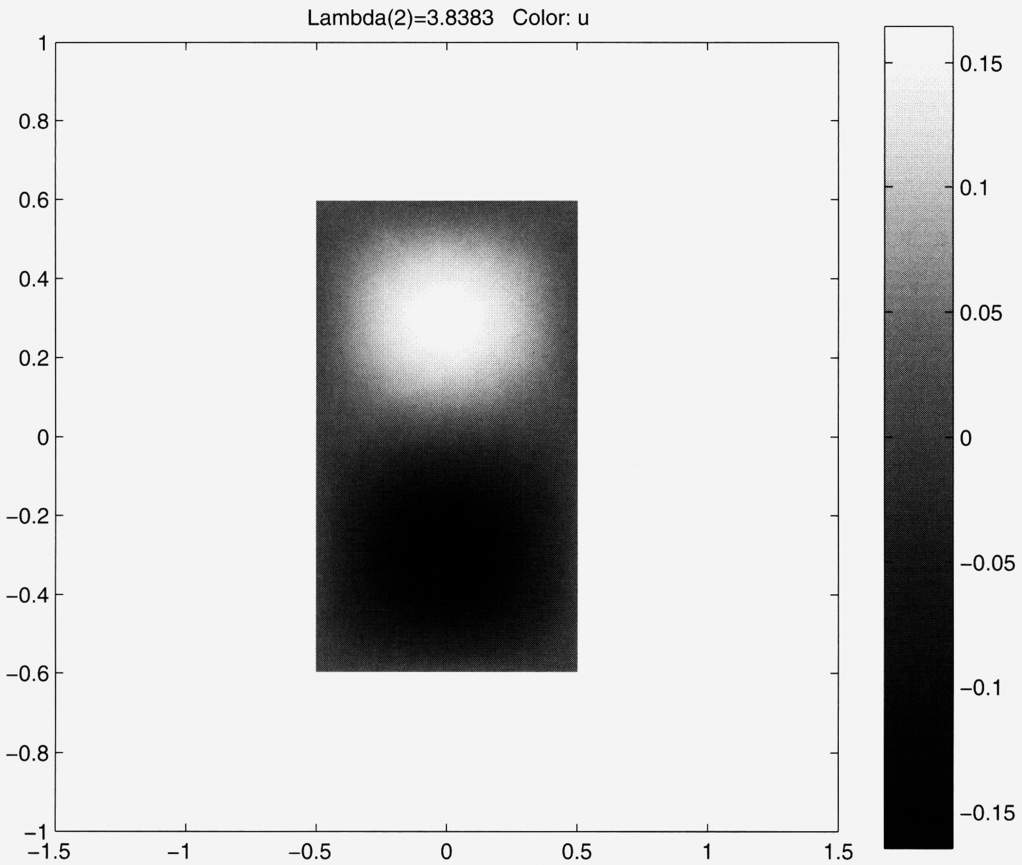

FIG. 3. Figure depicting the second eigenstate of the Laplacian for the unperturbed rectangle showing a horizontal nodal. In this n and the following three figures, the amplitude of the wavefunction is proportional to the degree of shading, given by the scale on the right.

the bounded concave elemental polygon-billiards. It is argued that the Lyapunov exponents for concave elemental polygon billiards go to zero with side curvature of the billiard. In the quantum domain, it is conjectured that a quantum number, $\mathbf{n_c}$, exists, above which quantum chaos develops. This parameter grows large as the side curvature of the concave billiards go to zero. For quantum numbers less than $\mathbf{n_c}$, the adiabatic theorem applies. A numerical study is included that lends support to this conjecture. It is shown also that eigenenergies of each of the four elemental quantum billiards behave proportionally to sE_1, where s is an integer and E_1 is a constant energy. Stemming from these observations, it is noted that quantum states of large quantum numbers have effective long-time behavior. This characteristic is found to imply a correspondence property between classical and quantum chaos for the concave elemental polygon quantum billiards.

Acknowledgments. Fruitful discussions on these topics with my colleagues Gregory Dionne, Joseph DiGioia, Joseph Greenberg, Joseph Salzman, and Gregory Ezra are

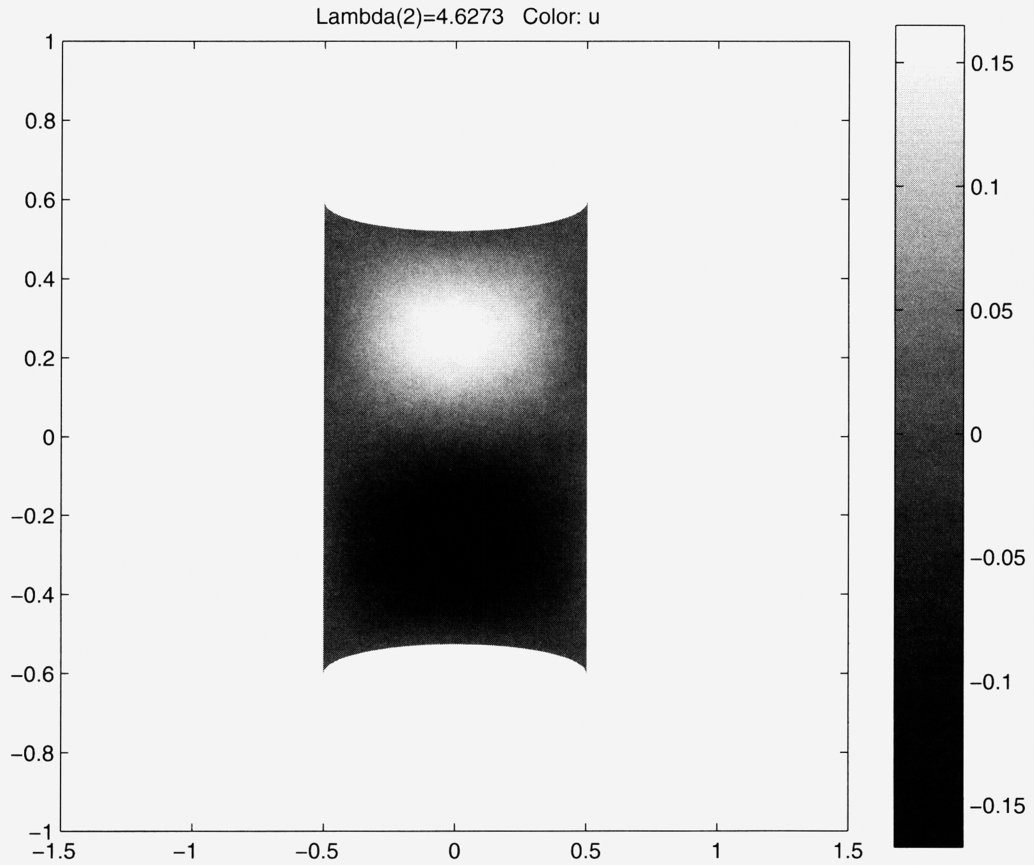

FIG. 4. Figure depicting the second eigenstate of the Laplacian for the perturbed rectangle again showing a horizontal nodal

gratefully acknowledged. I am particularly indebted to Mason Porter for assistance in numerical work for this study and his careful reading of this manuscript.

Appendix. In this appendix, the condition for the circular-configuration of maximum depression of side arms of respective elemental billiards is established. First we consider the square. It is shown that the maximum circular depression of an edge corresponds to the case of four contiguous circles whose tangent points form the square. The situation is shown in Fig.7. Let the square have edge-length a. From this figure one notes that the radius of curvature of an edge-segment arc is $\rho = a/\sqrt{2}$. One notes also that the depression of the mid-point of an edge Δ is given by

$$\Delta = a\left(\frac{1}{\sqrt{2}} - \frac{1}{2}\right) \approx 0.207a. \tag{A1}$$

It is noted that for any smaller radius of curvature, circles overlap within the square so that the given curvature is minimum. For a given square, the four circles that give this maximum depression are unique.

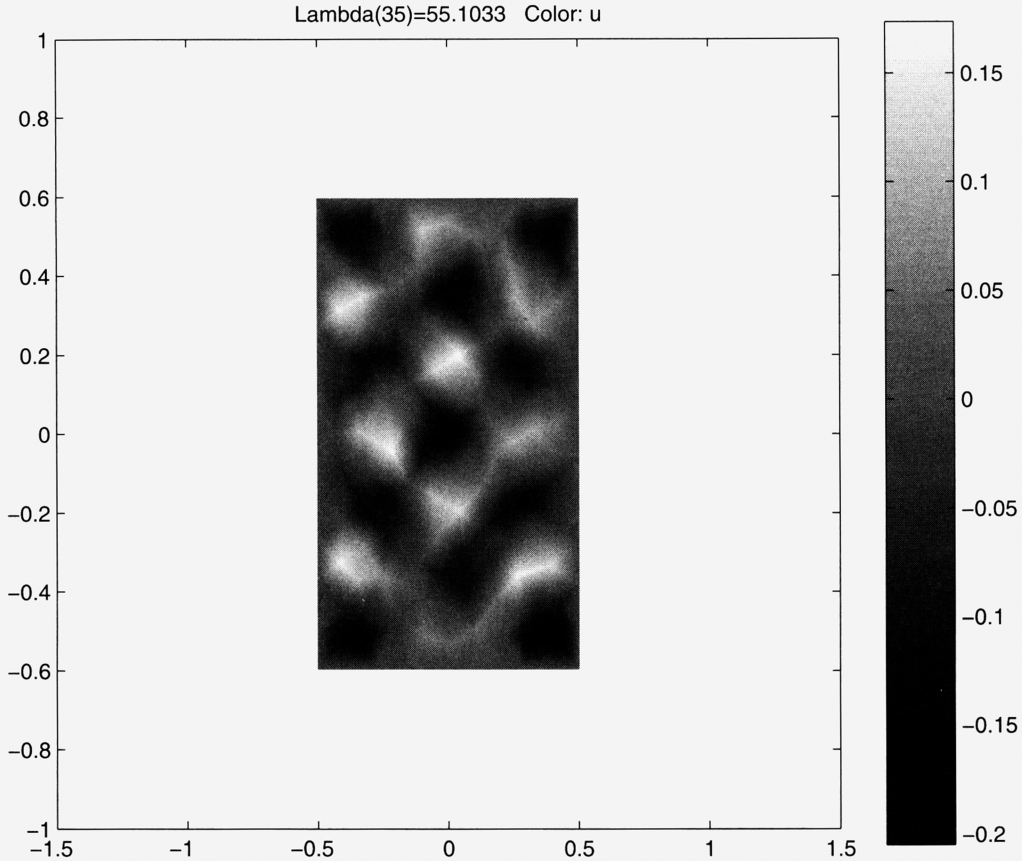

FIG. 5. Figure depicting 35th eigenstate of the Laplacian for the unperturbed rectangle showing an $x-y$ symmetry of its nodal structure

For the equilateral triangle, the circular configuration of maximum depression is shown in Fig. 8. With this figure one notes that the depression, Δ, is given by

$$\Delta = \frac{a}{2}\left(1 - \frac{\sqrt{3}}{2}\right) \approx 0.067a, \tag{A2}$$

where a is the length of a triangle leg. For this case, the radius of curvature, $\rho = a$.

It can be shown that the same contiguous circle configuration whose tangent points from either of the two remaining elemental polygons are likewise unique. For the isosceles right triangle, the related circular configuration of maximum depression consists of two congruent circles of a given radius and a third circle. The ratio of curvature of these two sets of circles is $1/\sqrt{2}$. For half the equilateral triangle billiard, the configuration of maximum depression consists of three circles of increasing radii of curvature in the ratio $1 : \sqrt{3} : 2$.

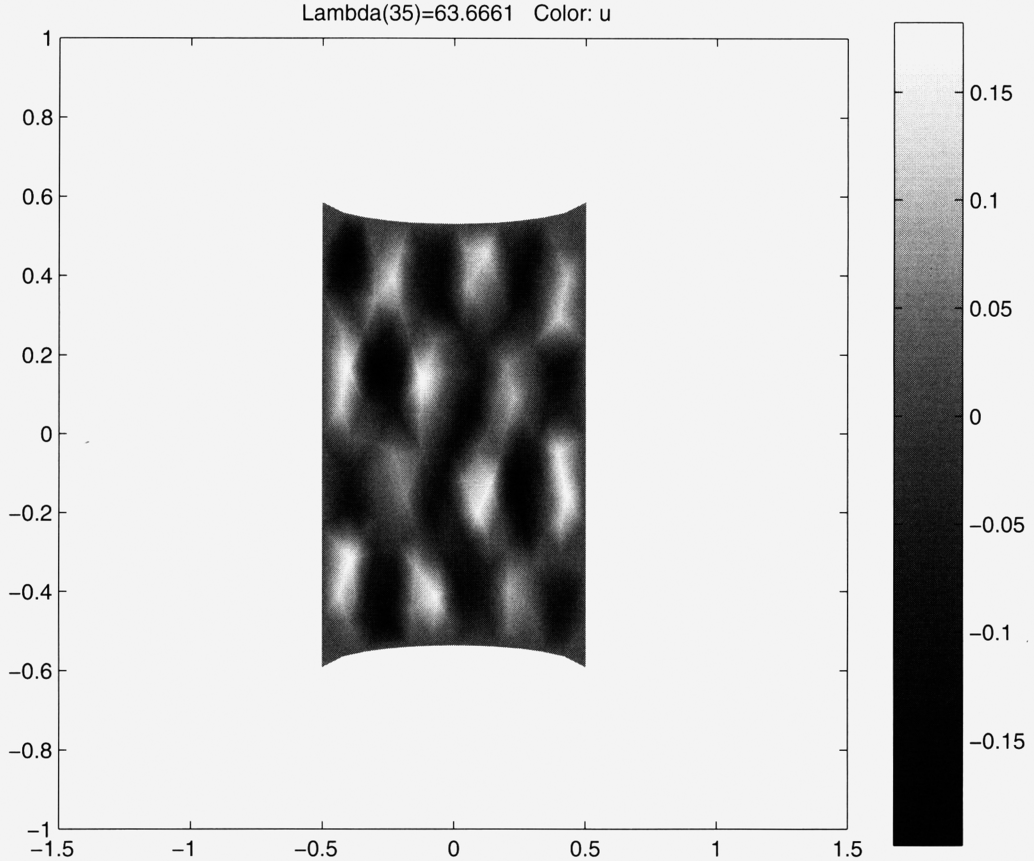

FIG. 6. Figure depicting 35th eigenstate of the Laplacian for the perturbed rectangle showing a loss of symmetry of the nodal structure of the unperturbed rectangle.

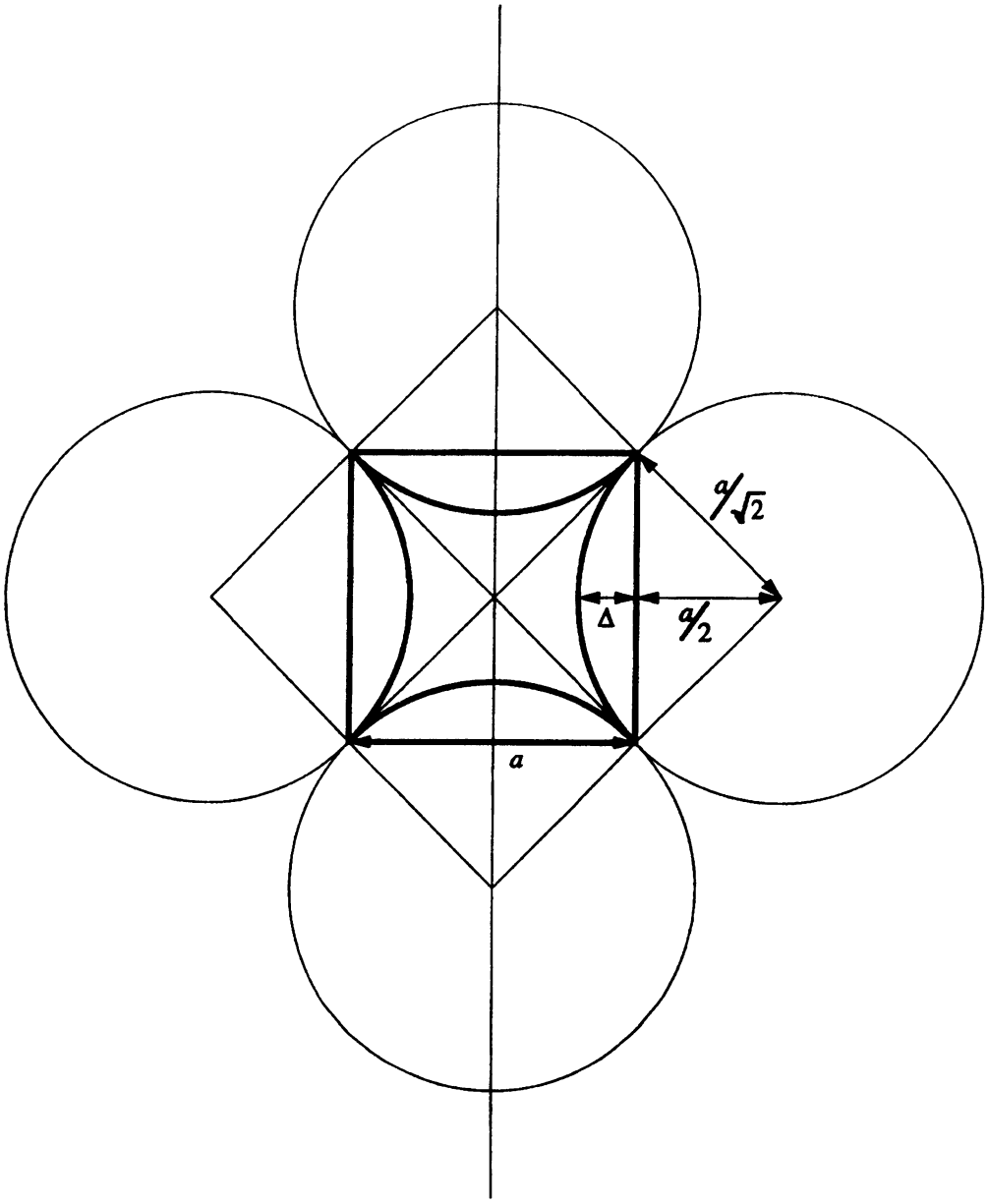

FIG. 7. A square whose corners are defined by the tangent points of the four contiguous congruent circles whose centers likewise form a square.

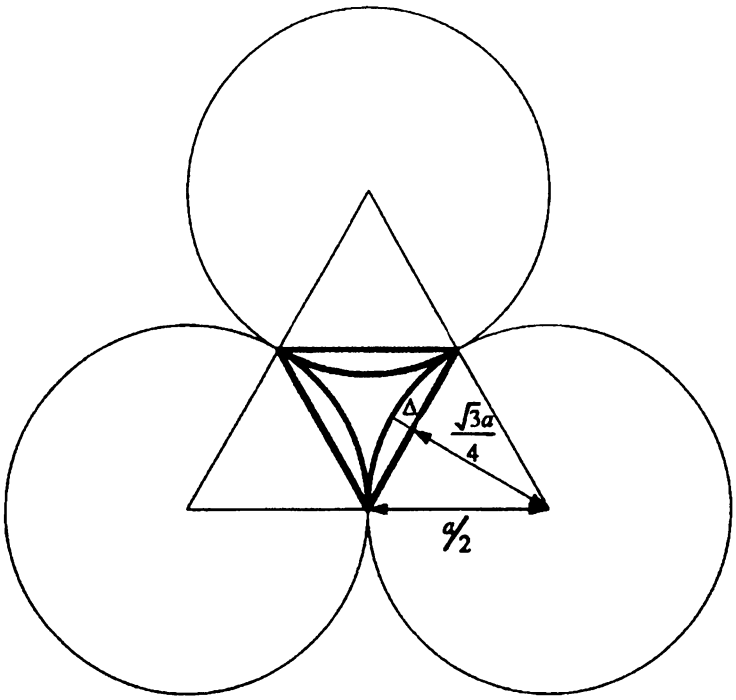

FIG. 8. An equilateral triangle whose corners are defined by the tangent points of the four contiguous congruent circles whose centers likewise form an equilateral triangle.

REFERENCES

[1] S. Kerckhoff, H. Masur, and J. Smillie, *Ergodicity of Billiard Flows and Quadratic-Differentials*, J. Ann. Math., **124** 293-311 (1986)
[2] Y. G. Sinai, *Introduction to Ergodic Theory*, Springer, New York (1976)
[3] I. P. Cornfield, S. V. Fomin, and Y. G. Sinai, *Ergodic Theory*, Springer, New York (1982)
[4] A. B. Katok and J. Strelcyn, *Invariant Manifolds, Entropy of Billiards*, Springer, New York (1986)
[5] V. Kozlov, *Billiards: A Generic Introduction to the Dynamics of Systems with Impacts*, AMS, Providence, RI (1991)
[6] R. L. Liboff, (a) *The Polygon Quantum Billiard*, J. Math. Phys. **35**, 596-607 (1994), (b) *Circular Sector Quantum Billiard and Allied Configurations*, J. Math. Phys. **35**, 2218-2228, (1994), (c) *Nodal-surface conjectures for the convex quantum billiard*, J. Math Phys. **35**, 3881-3886 (1994)
[7] V. Amar, M. Paupri, and A. Scotti, *Schrödinger Equation for Convex Plane Polygons: A Tiling Method for the Derivation of Eigenvalues and Eigenfunctions*, J. Math. Phys. **32**, 2442-2449 (1991)
[8] G. M. Zaslavsky, *Chaos in Dynamic Systems*, Harwood, New York (1985). In this work, the concave-segmented regular N-gon is labeled a 'star.' A rectangular billiard with a uniformly concave-segmented edge is labeled a 'caterpillar' billiard.
[9] M. C. Gurtzwiller, *Chaos in Classical and Quantum Mechanics*, Springer, New York, (1990)
[10] L. E. Reichl, *The Transition to Chaos*, Springer, New York (1992)
[11] E. Ott, *Chaos in Dynamical Systems*, Cambridge, New York (1993)
[12] M. Wojtkowski, *Principles for the Design of Billiards with Nonvanishing Lyapunov Exponents* Comm. Math. Phys. **105**, 391-414 (1986)
[13] G. Benettin, L. Galgani, and J. M. Strelcyn, Phys. Rev. **A14**, *Kolgomorov Entropy and Numerical experiments.* 2338-2345, (1976)

[14] M. Casartelli, E. Diana, I. Galgani, and A. Scotti, *Numerical Computations on a Stochastic Parameter Related to Kolgomorov Entropy*, Phys. Rev. **A13**, 1921-1295, (1976)
[15] A. Barnett, D. Cohen, and E. J. Heller, *Deformations and Dilations of Chaotic Billiards: Dissipation Rate and Quasiorthogonality of the Boundary Wave Functions*, Phys. Rev. Lett. **85**, 1412-1415 (2000)
[16] G. Cassati and T. Prosen, *Mixing Property of Triangular Billiards*, Phys. Rev. Lett. **83**, 4729-4732 (1999)
[17] R. L. Liboff, *Kinetic Theory: Classical, Quantum and Relativistic Descriptions*, 2nd ed., Wiley, New York (1998)
[18] C. Jaffe and W. P. Reinhardt, *Uniform Semiclassical Quantization of Regular and Chaotic Classical Dynamics on the Henon-Heiles Surface*, J. Chem. Phys. **77**, 5191-5203, (1982)
[19] R. B. Shirts and W. P. Reinhardt, *Approximate Constants of Motion for Classically Chaotic Vibrational Dynamics*, J. Chem. Phys. **77**, 5204-5217 (1982)
[20] K. Sohlberg and R. B. Shirts, *Semiclassical Quantization of a Nonintegrable System*, J. Chem. Phys. **101**, 7763-7778, (1994)
[21] N. Hungerbuehler, SIAM Review **42**, 657 (2000)
[22] R. Markarian, S-O. Kamphorst, and S. Carvallo, *A Lower Bound for Chaos on the Elliptical Stadium*, Physica **D115**, 189-202 (1998)
[23] H. Makino, T. Harayama, and Y. Aizawa, *Quantum-Classical Correspondences of the Berry-Robnik Parameter Through Bifurcations in Lemon Billiard Systems*, Phys. Rev. **E63**, Art. No. 056203 (2001)
[24] U. Krause, *Concave Perron-Frobenius Theory and Applications*, Nonlinear Analysis **47**, 1457–1466 (2001)
[25] J. Ding, *Absolutely Continuous Invariant Measure on a Piecewise Concave Mapping*, Nonlinear Analysis **28**, 1133-1140 (1997)
[26] Y. Zheng and J. F. Greenleaf, *The Effect of Concave and Convex Weight Adjustments on Self-Organizing Maps.* IEEE Transactions on Neural Networks **7**, 87-96 (1996)
[27] G. Benetin, *Power-Law Behavior of Lyapunov Exponents in Some Conservative Dynamical Systems*, Physica **D13**, 211-220 (1984)
[28] M. Wojtkowski, *Invariant Families of Cones and Lyapunov Exponents*, Ergodic Th. and Dynam. Sys. **8**, 145-161 (1985)
[29] R. Blümel and W. P. Reinhardt, *Chaos in Atomic Physics*, Cambridge, New York (1997)
[30] P. J. Richens and M. V. Berry, *Pseudointegrable systems in classical and quantum mechanics*, Physica **D2**, 495-412 (1981)
[31] B. Chirikov, F. Izrailev, and D. Shepelyansky, *Quantum chaos: Localization vs. Ergodicity*, Physica **D33**,77-88 (1988)
[32] R. L. Liboff, *The Many Faces of the Helmholtz Equation*, Phys. Essays **12**, 492 (1999)
[33] M. A. Pinsky, *The eigenvalues of an equilateral triangle*, Siam J. Math. Anal **11**, 819-949 (1980); **16**, 848 (1985)
[34] S. W. McDonald and A. N. Kaufman, *Wave chaos in the stadium*, Phys. Rev. **A37**, 3067-3078 (1988)
[35] G. Alessandrini, *Nodal lines of the fixed membrane problem in general convex domains*, Comm. Math. Helv. **69**, 142-154 (1994)
[36] R. L. Liboff, *Function-Mixing Hypothesis and Quantum Chaos*, Physica **D93**, 137 (1996)
[37] R. Courant and D. Hilbert, *Methods of Mathematical Physics*, vol 1, Interscience, New York (1966)
[38] R. L. Liboff, *Introductory Quantum Mechanics*, 3rd. ed., Addison Wesley, San Francisco (1998)
[39] L. Kaplan and E. J. Heller, *Weak Quantum Ergodicity*, Physica **D121**, 1-18, (1998)
[40] G. Casati, ed., *Chaotic Behavior in Quantum Systems*, Plenum, New York (1985)
[41] R. L. Liboff, *Bohr Correspondence Principle for Large Quantum Numbers*, Found. Phys. **5**, 271-293 (1975)